npj Precision Oncology

https://doi.org/10.1038/s41698-026-01350-z

Article in Press

SMARCA4/2 loss reduces BCL-xL expression and confers a druggable MCL1 dependency in cancer

Received: 9 October 2025

Accepted: 20 February 2026

Cite this article as: Jiang, J., Zhu, X., Fu, Z. *et al.* SMARCA4/2 loss reduces BCL-xL expression and confers a druggable MCL1 dependency in cancer. *npj Precis. Onc.* (2026). https://doi.org/10.1038/s41698-026-01350-z

Jialin Jiang, Xianbing Zhu, Zheng Fu, Minyan Lao, Azadeh Arabzadeh, Francis Robert, Anie Monast, Virginie Pilon, Kitty Pavlakis, Morag Park, William D. Foulkes & Sidong Huang

SMARCA4/2 loss reduces BCL-xL expression and confers a druggable MCL1 dependency in cancer

Jialin Jiang[1,2], Xianbing Zhu[1,2], Zheng Fu[1,2], Minyan Lao[1,2], Azadeh Arabzadeh[1,2], Francis Robert[1,2], Anie Monast[1,2], Virginie Pilon[1,2], Kitty Pavlakis[3], Morag Park[1,2, 4], William D. Foulkes[5,6,7], Sidong Huang[1, 2, 5§]

[1]Department of Biochemistry, McGill University, Montreal, QC, Canada.

[2]Rosalind & Morris Goodman Cancer Institute, McGill University, Montreal, QC, Canada.

[3]Department of Pathology, IASO women's hospital, Athens, Greece

[4]Department of Oncology, McGill University, Montreal, Canada

[5]Department of Human Genetics, McGill University, Montreal, Canada.

[6]SCCOHT/SMARCA4 Registry, Research Institute of the McGill University Health Centre, Montreal, Canada

[7]Department of Medical Genetics and Cancer Research Program, McGill University Health Centre, Montreal, Canada.

§ Corresponding author

Mailing addresses:

Department of Biochemistry, McGill University, McIntyre Medical Building, Room 810, 3655 Promenade Sir William Osler, Montreal, QC, H3G 1Y6, Canada

Phone: +1-514-660-0502

E-mail: sidong.huang@mcgill.ca

Running Title: SMARCA4/2 deficiency is synthetic lethal with MCL1 inhibition in cancers

Key words: SMARCA4/2, MCL1, BCL-xL, apoptosis, NSCLC, SCCOHT

ABSTRACT

SMARCA4 (BRG1) and SMARCA2 (BRM) are the mutually exclusive ATPase subunits of the SWI/SNF chromatin remodeling complexes often altered in cancers. Concurrent loss of SMARCA4/2 is found in some aggressive cancer types including small cell carcinoma of the ovary, hypercalcemic type (SCCOHT), a rare and lethal ovarian cancer affecting young women, and a subset of non-small cell lung cancers (NSCLCs), associated with chemotherapy resistance and poor outcome. Through a functional genetic approach, we identified that inhibition of MCL1, an anti-apoptotic protein of the BCL-2 family, is synthetic lethal with SMARCA4/2 loss in these cancer cells. MCL1 suppression by RNAi or a small molecule inhibitor, S63845, selectively induced apoptosis in SMARCA4/2-deficient SCCOHT and NSCLC cells but not in SMARCA4/2-proficient controls. Mechanistically, SMARCA4/2 directly promote mRNA expression of *BCL-xL*, encoding another key anti-apoptotic protein of the BCL-2 family; SMARCA4/2 loss therefore results in downregulation of BCL-xL leading to MCL dependency to suppress apoptosis in these cancer cells. Furthermore, single agent treatment of S63845 resulted in significant suppression of tumor growth in patient derived xenografts of SMARCA4/2-deficient NSCLC and SCCOHT. Collectively, our work uncovered MCL1 as a synthetic lethal target in SMARCA4/2-deficient cancers that may be exploited therapeutically.

Introduction

The switch/sucrose non-fermentable (SWI/SNF) complexes utilize chemical energy through ATP hydrolysis to remodel nucleosome positioning and conformation to control gene expression [1-3]. The abnormalities in different SWI/SNF subunits are implicated in the development of a broad range of human malignancies [4,5]. SMARCA4 and SMARCA2 are the two mutually exclusive SWI/SNF ATPases that are frequently altered in cancers. Inactivating *SMARCA4* mutations are found in ~7.2% of human cancers, including ~100% of small cell carcinoma of the ovary, hypercalcemic type (SCCOHT), a rare and aggressive ovarian cancer subtype and ~10% of non-small cell lung cancers (NSCLCs) [6-9]. In contrast, *SMARCA2* is often lost through epigenetic silencing, which is thought to cooperate with SMARCA4 deficiency for tumorigenesis in SCCOHT as well as in a subset of NSCLCs and other poorly differentiated aggressive cancers [10-15]. SMARCA4/2-deficient cancers often lack known druggable mutations and exhibit resistance to standard chemotherapy regimens, making them difficult to treat [6,16,17].

In search of alternative treatment strategies, previous studies have shown that SMARCA4/2-deficient cancers rely on epigenetic reprogramming and are responsive to inhibitors targeting the polycomb repressive complex 2, histone deacetylases, bromodomain-containing protein 4, and histone demethylase KDM6 in preclinical models [18-22]. We and others also found that these cancer cells are sensitive to drugs targeting receptor tyrosine kinases [23], CDK4/6 [24,25], arginine metabolism [26], as well as oxidative phosphorylation and glutamine metabolism [27]. However, most of these inhibitors primarily suppress proliferation, and drug resistance is expected to arise quickly - underscoring the need for novel therapeutic strategies that actively induce cancer cell death to achieve tumor eradication.

Anti-apoptotic proteins of the B-cell lymphoma-2 (BCL-2) family are promising therapeutic targets in cancer, as dysregulation of apoptosis – resulting from an imbalance between pro-apoptotic and anti-apoptotic factors - is a central hallmark of tumor development and progression [28-30]. Two key BCL-2 family proteins, myeloid cell leukemia sequence 1 (MCL1) and BCL2 Like 1 (BCL2L1, commonly referred to as BCL-x), coordinate in regulating BAK/BAX-dependent apoptosis and promoting cell survival [31-33]. MCL1 is anchored in the outer mitochondrial

membrane through its hydrophobic tail [34] and sequesters the proapoptotic proteins BAK/BAX via its hydrophobic groove in BCL-2 homology (BH) 3 domain [35]. BCL-x, encoded by the *BCL2L1* gene, has two isoforms produced through alternative splicing: BCL-xL and BCL-xS. The long isoform BCL-xL contains BH1-BH3 domains and exerts its anti-apoptotic function by inhibiting activation of BAX, like MCL1 [36,37]. In contrast, the short isoform BCL-xS is a pro-apoptotic protein – it lacks the BH1 and BH2 domains and binds to BCL-xL, causing the release of the pro-apoptotic BAK [38]. BCL-xL is the most abundant BCL-x protein in most cells. Overexpression of MCL1 and BCL-xL is widely observed in various cancers associated with poor prognosis and therapy resistance [39-41]. Therefore, a range of therapeutic agents targeting these anti-apoptotic proteins—such as small-molecule inhibitors (e.g., S63845 and Navitoclax)—have been developed to overcome resistance and improve clinical outcomes [42,43].

In this study, we uncovered that SMARCA4/2-deficient ovarian and lung cancer cells are selectively dependent on MCL1 through a systematic approach. We validated the selective MCL1 dependency in these cancer cells and tumors and uncovered the underlying mechanism, supporting MCL1 as a potential druggable target in SMARCA4/2-deficient cancers.

RESULTS

SMARCA4/2-deficient lung and ovarian cancer cells are selectively sensitive to MCL1 inhibition

To systematically uncover genetic vulnerabilities in SMARCA4/2-deficient cancer cells, we analyzed publicly available RNA-sequencing data from the Cancer Cell Line Encyclopedia (CCLE) [44,45] to stratify 111 ovarian and lung cancer cell lines into two groups based on *SMARCA4* mutation status and *SMARCA2* expression levels (see Methods). The lung cancer panel included 9 SMARCA4/2-deficient NSCLC cell lines [46] and 65 SMARCA4/2-proficient lines. The ovarian cancer cell line panel comprised 5 SMARCA4/2-deficient lines—including three SCCOHT cell lines (BIN-67, SCCOHT-1, and COV434) [14,47] and two dedifferentiated ovarian cancer lines (TOV-112D and OVK18) [20,47]—alongside 32 SMARCA4/2-proficient lines.

Next, we analyzed the genome-wide CRISPR/Cas9 knockout screens in these cell lines from the Cancer Dependency Map (DepMap, https://depmap.org) and used the ΔCERES (difference in the CERES scores), a metric that quantifies the difference in gene dependency between two cell line groups, to measure this selective lethality. We found that *MCL1*, but not other BCL-2 family members, was one of the top-ranked candidate genes whose knockout was selective lethal to SMARCA4/2-deficient cells in both cancer types (ΔCERES<-0.25, $-\log_{10}$(p-value)>2) (Fig. 1a and Supplementary Fig. 1), suggesting a unique role of MCL1 in promoting the survival of cancer cells with SMARCA4/2 loss. Furthermore, we queried the Genomics of Drug Sensitivity in Cancer (GDSC) database [48] for the available cell line drug response data corresponding to the lung and ovarian cancer cell lines used in the CCLE dataset in Figure 1a. Consistently, SMARCA4/2-deficient cells exhibited significantly lower half-maximal inhibitory concentrations (IC50) for three different MCL1 inhibitors (AZD5991, MIM1, and UMI-77) compared to SMARCA4/2-proficient cells (Fig. 1b). Together, these findings suggest that SMARCA4/2-deficient cancer cells are particularly vulnerable to MCL1 inhibition.

Validating this, knockdown of MCL1 using two independent shRNAs strongly suppressed growth in long-term colony formation assay in SMARCA4/2-deficient NSCLC cells (H1703) but had little effect on SMARCA4/2-proficient NSCLC cells (H1437) (Fig. 1c and Supplementary Data 1). As expected, MCL1 knockdown increased apoptosis as indicated by elevated levels of cleaved PARP (Fig. 1d). A similar trend was seen in ovarian cancer: SMARCA4/2-deficient SCCOHT cell lines, SCCOHT-1 and BIN-67, were much more sensitive to MCL1 knockdown compared to SMARCA4/2-proficient OVCAR4 high-grade serous carcinoma (HGSC) cells (Fig. 1e–f).

In line with the above RNAi results, the selective MCL1 inhibitor S63845 [42,49] elicited pronounced sensitivity in SMARCA4/2-deficient NSCLC lines (A427, H661, H1703, H23) compared to their proficient counterparts (H358, H1437, HCC827) in colony-formation and viability assays (Fig. 1g–h and Supplementary Data 1). Furthermore, S63845 treatment induced a partial but significant inhibition of tumor growth in a SMARCA4/2-deficient NSCLC patient-derived xenograft (PDX) model [27] (Fig. 1i and Supplementary Data 1). Similar results were also obtained in ovarian cancer models, where SMARCA4/2-deficient SCCOHT cells (COV434, SCCOHT-1, BIN-67) displayed marked sensitivity to S63845, contrasting with the reduced sensitivity of SMARCA4/2-proficient controls, including OVCAR4 and FT190, an immortalized but non-transformed fallopian cell line (Fig. 1j, k). Single agent treatment of S63845 also significantly suppressed the growth of SCCOHT xenografts *in vivo* (Fig. 1l). Together, these above data validated that SMARCA4/2-deficient cancer are vulnerable to MCL1 inhibition both *in vitro* and *in vivo*.

SMARCA4/2 loss causes the selective sensitivity to MCL1 inhibition

Our above results established the correlation of SMARCA4/2 deficiency and sensitivity to MCL1 inhibition. We next investigated whether SMARCA4/2 loss contributes to this selective dependency on MCL1 inhibition. Supporting this, re-expression of SMARCA4 in SMARCA4/2-

deficient A427 and H1703 NSCLC cells conferred resistance to S63845 in both cell viability and colony formation assays (Fig. 2a-d and Supplementary Data 1), which was accompanied with suppressed apoptosis as indicated by reduced expression of cleaved PARP upon S63845 treatment (Fig. 2e-f). In contrast to lung cancer cells, restoration of SMARCA4 in SCCOHT cells is known to cause strong growth repression [14,24], making long-term growth assays challenging. Nevertheless, short-term S63845 treatment assay also showed that ectopic SMARCA4 expression partially alleviated apoptosis induced by MCL1 inhibition (Fig. 2g). Conversely, CRISPR/Cas9-mediated *SMARCA4* knockout in SMARCA4/2-proficient FT190 and H1437 cells partially sensitized them to S63845 although not statistically significant, and *SMARCA2* knockdown using two independent shRNAs in these *SMARCA4* knockout cells further increased their drug sensitivities (Supplementary Fig. 2 and Supplementary Data 1). Notably, SMARCA4 knockout in these cells resulted in reduced SMARCA2 expression, which requires further investigations but nevertheless supports the causal role of these two paralogs in regulating S63845 sensitivity. Taken together, these data indicate that SMARCA4/2 loss in lung and ovarian cancer cells results in selective sensitivity to MCL1 inhibition, at least partly mediated through enhanced apoptosis.

SMARCA4/2 loss results in BCL-xL deficiency

Next, we investigated the mechanism underlying this selective MCL1 dependency of SMARCA4/2 loss. Given the well-established role of MCL1 in apoptosis control and SMARCA4/2 in gene expression regulation, we hypothesized that SMARCA4/2 loss may result in either aberrant MCL1 expression or dysregulation of other BCL-2 members leading to MCL1 dependency. To investigate this, we analyzed RNA-seq datasets from SMARCA4/2-proficient NSCLC H358 cells to profile BCL-2 family gene expression before and after SMARCA4 knockdown [50]. In parallel, we also examined how restoring SMARCA4 or SMARCA2 affected the expression of these genes in SMARCA4/2-deficient models, including NSCLC (A427, H1703) and SCCOHT (COV434, SCCOHT-1, BIN-67) cell lines [24,51]. As shown in Figure 3a, among the 12 key BCL-2 family members, *BCL2L1* was the only gene obviously regulated by SMARCA4 or

SMARCA2 across all cell lines – downregulated upon SMARCA4 knockdown and upregulated upon restoration of SMARCA4 or SMARCA2, whereas MCL1 expression remained largely unaffected.

BCL2L1 encodes BCL-xL and BCL-xS isoforms that arise from alternative splicing and have opposing functions in inhibiting and promoting apoptosis, respectively [52]. Closer examination of the RNA-seq data showed that the dominant isoform in BIN-67 cells is *BCL-xL*, which was upregulated upon SMARCA4 restoration and was ~ 40 folds more abundant than *BCL-xS* (Supplementary Fig. 3a, b). Given that *BCL2*, another key anti-apoptotic protein, was also expressed at low levels among all cell lines independent of SMARCA4/2 status (Fig 3a), these observations highlight the potential key role of *BCL2L1* regulation by SMARCA4/2 in this context of MCL1 dependency. In line with these cell lines data, analysis of the RNA-seq datasets of SCCOHT [17] and TCGA HGSC tumors [53] showed that SCCOHT tumors expressed significantly lower *BCL2L1* than HGSCs (Fig. 3b). These observations suggest that SMARCA4/2 loss causes reduced BCL-xL expression leading to increased dependency on MCL1 in these cancer cells to suppress apoptosis.

Further supporting the regulation of BCL-xL by SMARCA4/2, ectopic expression of SMARCA4 in SMARCA4/2-deficient SCCOHT and NSCLC cell lines significantly increased *BCL-xL* mRNA levels, as shown by qPCR (Fig. 3c and Supplementary Fig. 3c), and concurrently a trend of BCL-xL protein level elevation (Fig. 3d). Moreover, analysis of a panel of 21 NSCLC cell lines revealed a positive correlation between SMARCA4/2 expression status and BCL-xL protein levels (Fig. 3e and Supplementary Fig. 4) - while SMARCA4/2-deficient cells exhibited the lowest BCL-xL expression, among SMARCA4-deficient lines that retain SMARCA2 expression, BCL-xL expression positively correlated with SMARCA2 levels, which is in line with the functional redundancy between SMARCA4 and SMARCA2 in regulating *BCL-xL* expression (Fig. 3c). Together, these results indicate that SMARCA4/2 loss results in reduced *BCL2L1* expression leading to BCL-xL reduction, which may underlie MCL1 dependency.

SMARCA4/2 directly controls chromatin accessibility of the BCL2L1 locus

Given the chromatin remodeling role of SWI/SNF, we also examined the chromatin architecture of the *BCL2L1* locus and its potential direct regulation by SMARCA4/2. Indeed, upon SMARCA4 restoration, ChIP-seq analysis in BIN-67 cells [51] revealed SMARCA4 occupancy at the promoter and regulatory regions of *BCL2L1* (Fig. 3f), suggesting that SMARCA4 directly regulates *BCL2L1* expression. Supporting this, we found that ChIP-seq signals of H3K27Ac, a chromatin mark associated with active promoters and enhancers, were elevated at these regions upon re-expression of SMARCA4 or SMARCA2 in both BIN-67 and H1703 cells [25]. In addition, the Assay for Transposase-Accessible Chromatin using sequencing (ATAC-seq) peaks at these genomic regions were also elevated upon restoration of SMARCA4 or SMARCA2 in BIN-67 and H1703 cells (Fig. 3f), indicating enhanced chromatin accessibility at the *BCL2L1* locus when SMARCA4/2 was present. These data support a model in which SMARCA4/2 promote *BCL2L1* transcription by directly remodeling chromatin structure at its gene locus.

BCL-xL deficiency underlies the synthetic lethal interaction between MCL1 inhibition and SMARCA4/2 loss

Our data thus far suggest that SMARCA4/2 loss leads to reduced BCL-xL expression, which could limit the total anti-apoptotic capacity in SMARCA4/2-deficient cancer cells and renders their sensitivity to MCL1 inhibition. If this hypothesis is correct, forced elevation of BCL-xL should rescue these cancer cells from MCL1 inhibition. Indeed, ectopic expression of BCL-xL conferred resistance to S63845 treatment in H1703 and SCCOHT-1 cells in both colony-formation and cell viability assays (Fig. 4a-d and Supplementary Data 1) and suppressed apoptosis induction (Fig. 4e-f). MCL1 overexpression also yielded a similar phenotype, although the effect was less pronounced at higher concentrations of S63845. This is expected, as S63845 targets MCL1, and higher concentrations of the drug may saturate the available MCL1 pool. Similarly, ectopic expression of BCL-xL protected H1703 cells from the growth inhibition and apoptosis induction

caused by a shRNA targeting the 3′UTR of *MCL1* (Fig. 4g-h and Supplementary Data 1). As a control, ectopic expression of an *MCL1* cDNA lacking 3′UTR also rescued these phenotypes induced by this shRNA against *MCL1* (Fig. 4g-h and Supplementary Data 1).

While our above data established that reduced BCL-xL expression in SMARCA4/2-deficient cancer cells contributes to their increased dependency on MCL1 for apoptosis inhibition, it remained unclear if this is the main cause since SMARCA4/2 regulate expression of diverse genes and pathways. To test this, we took advantage of the fact that SMARCA4/2-deficient NSCLC cells can better tolerate restoration of SMARCA4 and performed "double rescue" experiments. As shown in Figure 4i, while restoration of SMARCA4 in both A427 and H1703 cells conferred resistance to MCL1 inhibition by S63845, addition of WEHI-539, a selective BCL-xL inhibitor, completely reversed their sensitivity to S63845. Importantly, WEHI-539 treatment alone did not suppress the growth of the cells. These results indicate that reduced BCL-xL expression in SMARCA4/2-deficient cancer cells is the main underlying cause for their dependency on MCL1 (Supplementary Fig. 5).

DISCUSSION

In this study, we identified and validated MCL1 as a druggable dependency in SMARCA4/2-deficient ovarian and lung cancers. We demonstrated that this selective MCL1 dependency is associated with the downregulation of BCL-xL induced by SMARCA4/2 loss and may be exploited therapeutically using MCL1 inhibitors.

MCL1/BCL-xL ratio has been previously shown to predict the efficiency of MCL1 inhibition in NSCLC cell lines, although the genetic events causing this MCL1/BCL-xL imbalance were not known [54]. Our findings are in line with this study and provide the mechanistic link between SMARCA4/2 deficiency and altered MCL1/BCL-xL ratio. We demonstrated that SMARCA4/2 directly regulate *BCL-xL* mRNA expression and SMARCA4/2 loss thus results in BCL-xL deficiency leading to MCL1 dependency in both SCCOHT and NSCLC cells. While SMARCA4 has been shown to influence splicing programs, no differential BCL2L1 (BCL-x) splicing upon SMARCA4 perturbation was detected [55]. Consistent with this, SMARCA4 restoration in SCCOHT cells increased mRNA expression of both isoforms, with BCL-xL being the dominant isoform expressed in these cancer cells. Forced re-expression of SMARCA4 conferred resistance to MCL1 inhibition in SMARCA4/2-deficient cancer cells. This resistance was reversed by co-treatment with a selective BCL-xL inhibitor. supporting the causal role of reduced BCL-xL expression in mediating the synthetic lethal interaction between SMARCA4/2 loss and MCL1 inhibition.

The MCL1 inhibitor S63845 has demonstrated significant anti-tumor activity in models of multiple myeloma, lymphoma, and myeloid leukemia, where 45-68% of cell lines tested exhibited high sensitivity to S63845 (IC_{50}<0.1μM) [42,56]. Its derivative, S64315, is currently being evaluated in clinical trials for these hematologic malignancies [56]. While our results showed that S63845 was also highly effective in targeting SMARCA4/2-deficient SCCOHT and NSCLC cells *in vitro* (IC_{50}<0.1μM), it had modest anti-tumor activity *in vivo* against the PDX models. Future studies with SMARCA4/2-proficeint models as controls may help better establish this potential utility of S63845 for SMARCA4/2-deficient tumors. This modest *in vivo* anti-tumor activity of S63845 could be potentially attributed to limited drug penetration due to the compactness of the solid tumor in contrast to leukemic cancers. Treatment strategies combining MCL1 inhibitor and other agents

may help overcome this and enhance its clinical utility. In fact, S63845 is mostly used in combination with other drugs, such as nucleoside azacitidine [57] and BCL-2 inhibitor venetoclax [58]. Notably, our previous study demonstrated that the loss of SMARCA4/2 confers chemotherapy-induced apoptosis in lung and ovarian cancers due to downregulation of ITPR3, a critical ion channel that mediates Ca^{2+} flux from the endoplasmic reticulum to mitochondria—a process essential for apoptosis induction [17]. Therefore, combining cisplatin with an MCL1 inhibitor may enhance tumor cell sensitivity by promoting apoptosis in these SMARCA4/2-deficient cancers with BCL-xL deficiency. Notably, a previous study reported that separase-dependent cleavage of MCL1 and BCL-xL can induce apoptosis and cell death in shortened mitosis, indicating that these factors also participate in cell cycle regulation [59]. Thus, combined MCL1 and CDK4/6 inhibitors may have a synergistic effect targeting SMARCA4/2-deficient cancers. Given that CDK4/6 have been shown to be effective in suppressing preclinical models of these SWI/SNF-deficient cancers [24,25,60], such potential combination strategies warrant future investigations.

In summary, our study uncovered MCL1 as a synthetic lethal target in SMARCA4/2-deficient lung and ovarian cancers. Given the clinical advancement of MCL1 inhibitors in hematologic malignancies, MCL1 inhibition may also be considered for the treatment of SMARCA4/2-deficient cancers.

Methods

Cell culture Cells were cultured in Dulbecco's modified Eagle medium (Thermo Fisher Scientific, 11995-065) or Roswell Park Memorial Institute 1640 Medium (Thermo Fisher Scientific, Cat# 11875-093) supplemented with 7% fetal bovine serum (Sigma, Cat# F1051), 2 mM L-glutamine (Thermo Fisher Scientific, 25030-081), and 1% penicillin/streptomycin (Thermo Fisher Scientific, 15140-122) at 37°C and 5% CO_2. Mycoplasma contamination was routinely tested using MycoAlert (Lonza, LT07-318). Short tandem repeat (STR) profiling confirmed cell line identity.

Compounds and antibodies S63845 (HY-100741) and WEHI-539 (HY-15607) were from MedChemExpress. Antibodies against β-Actin (sc-47778), HSP90 (sc-13119), SMARCA2 (11996), MCL1 (94296S), BCL-xL (2764), cleaved PARP (5625), and cleaved caspase-3 (9664) were used at 1:1000; SMARCA4 (A300-813A) was used at 1:5000.

Plasmids and lentiviral transduction shRNAs and ORFs were from the Mission TRC library (Sigma) via McGill Genetic Perturbation Service (GPS) and McGill Platform for Cellular Perturbation (MPCP). Constructs included shMCL1#1 (TRCN0000196390), shMCL1#2 (TRCN0000197024), pLKO_TRC001, pReceiver-Lv105, pReceiver-SMARCA4 (GeneCopoeia), and pLX304 vectors (*MCL1* ccsbBroad304_00985, *BCL-xL* CCSBBroad304_053D1_C02, *GFP* ccsbBroad304_07515; Transomic). Lentivirus was produced in 293T cells via $CaCl_2$-mediated transfection with psPAX2 and pMD2.G. Supernatants were harvested 24 and 36 h post-transfection and used to infect target cells. Selection was done with puromycin (2 μg/mL) or blasticidin (20 μg/mL) for 2–4 days.

RNA isolation and qRT-PCR Trizol (Invitrogen) was used to isolate total mRNA and Maxima First Strand cDNA Synthesis Kit (Thermo Scientific) was used to convert mRNA to cDNA. qRT-PCR (Quantitative real-time reverse transcription PCR) was performed using SYBR® Green master mix (Roche) according to manufacturer's protocol. Relative mRNA levels of indicated genes were determined by normalizing to the housekeeping gene *ACTB*. The sequences of the qRT-PCR primers are as follows: ACTB_Forward (Fwd), GTTGTCGACGACGAGCG;

ACTB_Reverse (Rev), GCACAGAGCCTCGCCTT; BCL-xL Forward (Fwd), CCTAAGGCGGATTTGAATAATCTT; BCL-xL Reverse (Rev), CCCGGTTGCTCTGAGACATT.

Colony formation assay Cells (2–8 × 10^4/well) were seeded in 6-well plates. Drugs or vehicle were added the next day and refreshed every 3 days for 10–14 days. Colonies were fixed in 3.75% formaldehyde, stained with 0.1% crystal violet. All colony formation assays were independently reproduced at least two to three times and quantified by ImageJ plugin ColonyArea (https://github.com/Turku-BioImaging/ColonyArea) as shown in Supplementary Data 1.

Cell viability assay Cells (1,000–6,000/well) were plated in 96-well plates and treated after 24 hours with compound dilutions. After 4 days, viability was measured by CellTiter-Blue (Promega) at 560/590 nm in a Tecan Infinite M200 PRO multimode microplate reader. Data were normalized to vehicle controls.

Immunoblotting Cells were lysed in SDS buffer 24 h post-treatment. Lysates were separated using NuPAGE gels (Thermo Fisher) and transferred to membranes. β-Actin and HSP90 served as loading controls. Uncropped scans of western blots are shown in Supplementary Figure 6.

Transcriptome and chromatin profiling RNA-seq, ATAC-seq, and ChIP-seq data were obtained from GSE151026, GSE117735, GSE121755, and GSE162611. Reads were aligned to hg19 using STAR (v2.6.1c) [61] and quantified using featureCounts (v1.6.4) [62]. IGV [63] was used for visualization. RNA-seq read counts from 13 SCCOHT tumors [17,64] and 379 ovarian cancer tumors retrieved from UCSC Xena (http://xena.ucsc.edu/) were processed uniformly using the same computational pipeline. The fragments per kilobase of transcript per million mapped reads (FPKM) values were calculated as (RCg × 10^9)/(RCpc × L), in which RCg is the number of reads mapped to the gene; RCpc is the number of reads mapped to protein-coding genes; and L is mean of lengths of the gene isoforms. ggplot2 (v3.3.3) [65] was used for visualization. Cell lines were defined as *SMARCA4/2*-dual deficient according to literature references (SCCOHT-1, COV434, BIN-67, TOV112D, OVK18, H1703, A427, H522, H23) [46] or if the cell lines displayed damaging mutations on *SMARCA4* and low *SMARCA2* expression (Log_2(TPM+1) <3). Isoform-level quantification of

BCL-xL and *BCL-xS* from the RNA-seq dataset in BIN-67 cells (GSE151026) was conducted: reads were aligned to hg19 with STAR and transcript abundances were normalized to total counts per sample to generate counts per million (CPM). A Sashimi plot was generated to visualize alternative splicing (AS) pattern of the *BCL2L1* gene.

In vivo experiments PDX tumors (NRTO-1, TM01563) were implanted in NSG mice. Mice (n=3–5/group) received vehicle or 25 mg/kg S63845 (intraperitoneal injection) twice weekly. S63845 was dissolved in 25 mM HCl and 20% hydroxypropyl-β-cyclodextrin. Tumor size was measured twice weekly by blinded assessors. Procedures were approved by the McGill Animal Care Committee.

Statistical analysis Statistical significance was tested using unpaired two-tailed Student's *t*-test when comparing two groups, and one-way analysis of variance (ANOVA) with Dunnett's post hoc test for multiple groups. *p*-values: **p*<0.05, ***p*<0.01, ****p*<0.001, *****p*<0.0001. Graphs represent mean values and error bars represent ± standard deviation (s.d.).

Data availability

DepMap CRISPR screen: https://depmap.org/portal/. Gene expression/mutation: CCLE (https://portals.broadinstitute.org/ccle), UCSC Xena (http://xena.ucsc.edu/). Drug response: GDSC (https://www.cancerrxgene.org/). Dependency scores: CERES. Public datasets: GSE151026 [51], GSE117735 [66], GSE121755 [25], GSE162611 [50].

Code availability

All analyses were conducted in R using standard packages for data visualization and statistics. No custom algorithms were developed. The code and analysis scripts are available upon request.

Acknowledgements

This work was supported by Canadian Institute of Health Research (CIHR) grants PJT-156233 (S.H.), PJT-438303 (S.H.), PJT- 518050 (S.H.), and FDN-148390 (W.D.F). S.H. was supported by a Canada Research Chair in Functional Genomics.

Author Contribution

J.J., X. Zhu., Z.F., M.L., A.A., A.M., and V.P. carried out experiments and data analysis. J.J. and X. Zhu. performed statistical and bioinformatic analysis. F.R. and K.P. contributed expertise and samples. M.P., W.D.F., and S.H. supervised the experiments. S.H. conceived and oversaw the study. J.J. and S.H. wrote the manuscript. All authors reviewed the manuscript.

Competing Interest Statement

The authors declare no competing interests.

REFERENCE

1 Kadoch, C. & Crabtree, G. R. Mammalian SWI/SNF chromatin remodeling complexes and cancer: Mechanistic insights gained from human genomics. *Sci Adv* **1**, e1500447 (2015). https://doi.org/10.1126/sciadv.1500447

2 Pan, J. *et al.* Interrogation of Mammalian Protein Complex Structure, Function, and Membership Using Genome-Scale Fitness Screens. *Cell Syst* **6**, 555-568 e557 (2018). https://doi.org/10.1016/j.cels.2018.04.011

3 Reisman, D., Glaros, S. & Thompson, E. A. The SWI/SNF complex and cancer. *Oncogene* **28**, 1653-1668 (2009). https://doi.org/10.1038/onc.2009.4

4 Kadoch, C. *et al.* Proteomic and bioinformatic analysis of mammalian SWI/SNF complexes identifies extensive roles in human malignancy. *Nat Genet* **45**, 592-601 (2013). https://doi.org/10.1038/ng.2628

5 Shain, A. H. & Pollack, J. R. The spectrum of SWI/SNF mutations, ubiquitous in human cancers. *PLoS ONE* **8**, e55119 (2013). https://doi.org/10.1371/journal.pone.0055119

6 Tischkowitz, M. *et al.* Small-Cell Carcinoma of the Ovary, Hypercalcemic Type-Genetics, New Treatment Targets, and Current Management Guidelines. *Clin Cancer Res* **26**, 3908-3917 (2020). https://doi.org/10.1158/1078-0432.CCR-19-3797

7 Jelinic, P. *et al.* Recurrent SMARCA4 mutations in small cell carcinoma of the ovary. *Nat Genet* **46**, 424-426 (2014). https://doi.org/10.1038/ng.2922

8 Ramos, P. *et al.* Small cell carcinoma of the ovary, hypercalcemic type, displays frequent inactivating germline and somatic mutations in SMARCA4. *Nat Genet* **46**, 427-429 (2014). https://doi.org/10.1038/ng.2928

9 Witkowski, L. *et al.* Germline and somatic SMARCA4 mutations characterize small cell carcinoma of the ovary, hypercalcemic type. *Nat Genet* **46**, 438-443 (2014). https://doi.org/10.1038/ng.2931

10 Matsubara, D. *et al.* Lung cancer with loss of BRG1/BRM, shows epithelial mesenchymal transition phenotype and distinct histologic and genetic features. *Cancer Sci* **104**, 266-273 (2013). https://doi.org/10.1111/cas.12065

11 Reisman, D. N., Sciarrotta, J., Wang, W., Funkhouser, W. K. & Weissman, B. E. Loss of BRG1/BRM in human lung cancer cell lines and primary lung cancers: correlation with poor prognosis. *Cancer Res* **63**, 560-566 (2003).

12 Estel, R., Hackethal, A., Kalder, M. & Munstedt, K. Small cell carcinoma of the ovary of the hypercalcaemic type: an analysis of clinical and prognostic aspects of a rare disease on the basis of cases published in the literature. *Arch Gynecol Obstet* **284**, 1277-1282 (2011). https://doi.org/10.1007/s00404-011-1846-5

13 Jelinic, P. *et al.* Concomitant loss of SMARCA2 and SMARCA4 expression in small cell carcinoma of the ovary, hypercalcemic type. *Mod Pathol* **29**, 60-66 (2016). https://doi.org/10.1038/modpathol.2015.129

14 Karnezis, A. N. *et al.* Dual loss of the SWI/SNF complex ATPases SMARCA4/BRG1 and SMARCA2/BRM is highly sensitive and specific for small cell carcinoma of the ovary, hypercalcaemic type. *J Pathol* **238**, 389-400 (2016). https://doi.org/10.1002/path.4633

15 Karnezis, A. N., Cho, K. R., Gilks, C. B., Pearce, C. L. & Huntsman, D. G. The disparate origins of ovarian cancers: pathogenesis and prevention strategies. *Nat Rev Cancer* **17**, 65-74 (2017). https://doi.org/10.1038/nrc.2016.113

16 Witkowski, L. *et al.* The influence of clinical and genetic factors on patient outcome in small cell carcinoma of the ovary, hypercalcemic type. *Gynecol Oncol* **141**, 454-460 (2016).

https://doi.org/10.1016/j.ygyno.2016.03.013

17 Xue, Y. *et al.* SMARCA4/2 loss inhibits chemotherapy-induced apoptosis by restricting IP3R3-mediated Ca(2+) flux to mitochondria. *Nat Commun* **12**, 5404 (2021). https://doi.org/10.1038/s41467-021-25260-9

18 Wang, Y. *et al.* Histone Deacetylase Inhibitors Synergize with Catalytic Inhibitors of EZH2 to Exhibit Antitumor Activity in Small Cell Carcinoma of the Ovary, Hypercalcemic Type. *Mol Cancer Ther* **17**, 2767-2779 (2018). https://doi.org/10.1158/1535-7163.MCT-18-0348

19 Wang, Y. *et al.* The histone methyltransferase EZH2 is a therapeutic target in small cell carcinoma of the ovary, hypercalcaemic type. *J Pathol* **242**, 371-383 (2017). https://doi.org/10.1002/path.4912

20 Chan-Penebre, E. *et al.* Selective Killing of SMARCA2- and SMARCA4-deficient Small Cell Carcinoma of the Ovary, Hypercalcemic Type Cells by Inhibition of EZH2: In Vitro and In Vivo Preclinical Models. *Mol Cancer Ther* **16**, 850-860 (2017). https://doi.org/10.1158/1535-7163.MCT-16-0678

21 Shorstova, T. *et al.* SWI/SNF-Compromised Cancers Are Susceptible to Bromodomain Inhibitors. *Cancer Res* **79**, 2761-2774 (2019). https://doi.org/10.1158/0008-5472.CAN-18-1545

22 Romero, O. A. *et al.* SMARCA4 deficient tumours are vulnerable to KDM6A/UTX and KDM6B/JMJD3 blockade. *Nat Commun* **12**, 4319 (2021). https://doi.org/10.1038/s41467-021-24618-3

23 Lang, J. D. *et al.* Ponatinib Shows Potent Antitumor Activity in Small Cell Carcinoma of the Ovary Hypercalcemic Type (SCCOHT) through Multikinase Inhibition. *Clin Cancer Res* **24**, 1932-1943 (2018). https://doi.org/10.1158/1078-0432.CCR-17-1928

24 Xue, Y. *et al.* CDK4/6 inhibitors target SMARCA4-determined cyclin D1 deficiency in hypercalcemic small cell carcinoma of the ovary. *Nat Commun* **10**, 558 (2019). https://doi.org/10.1038/s41467-018-06958-9

25 Xue, Y. *et al.* SMARCA4 loss is synthetic lethal with CDK4/6 inhibition in non-small cell lung cancer. *Nat Commun* **10**, 557 (2019). https://doi.org/10.1038/s41467-019-08380-1

26 Ji, J. X. *et al.* Arginine depletion therapy with ADI-PEG20 limits tumor growth in argininosuccinate synthase deficient ovarian cancer, including small cell carcinoma of the ovary, hypercalcemic type. *Clin Cancer Res* (2020). https://doi.org/10.1158/1078-0432.CCR-19-1905

27 Zhu, X. *et al.* Alanine supplementation exploits glutamine dependency induced by SMARCA4/2-loss. *Nat Commun* **14**, 2894 (2023). https://doi.org/10.1038/s41467-023-38594-3

28 Plati, J., Bucur, O. & Khosravi-Far, R. Dysregulation of apoptotic signaling in cancer: molecular mechanisms and therapeutic opportunities. *J Cell Biochem* **104**, 1124-1149 (2008). https://doi.org/10.1002/jcb.21707

29 Ashkenazi, A., Fairbrother, W. J., Leverson, J. D. & Souers, A. J. From basic apoptosis discoveries to advanced selective BCL-2 family inhibitors. *Nat Rev Drug Discov* **16**, 273-284 (2017). https://doi.org/10.1038/nrd.2016.253

30 Kale, J., Osterlund, E. J. & Andrews, D. W. BCL-2 family proteins: changing partners in the dance towards death. *Cell Death Differ* **25**, 65-80 (2018). https://doi.org/10.1038/cdd.2017.186

31 Huang, K. *et al.* BH3-only proteins target BCL-xL/MCL-1, not BAX/BAK, to initiate apoptosis. *Cell Res* **29**, 942-952 (2019). https://doi.org/10.1038/s41422-019-0231-y

32 Debrincat, M. A. *et al.* Mcl-1 and Bcl-x(L) coordinately regulate megakaryocyte survival. *Blood* **119**, 5850-5858 (2012). https://doi.org/10.1182/blood-2011-12-398834

33 Kodama, T. *et al.* Mcl-1 and Bcl-xL regulate Bak/Bax-dependent apoptosis of the megakaryocytic lineage at multistages. *Cell Death Differ* **19**, 1856-1869 (2012). https://doi.org/10.1038/cdd.2012.88

34 Perciavalle, R. M. & Opferman, J. T. Delving deeper: MCL-1's contributions to normal and cancer biology. *Trends Cell Biol* **23**, 22-29 (2013). https://doi.org/10.1016/j.tcb.2012.08.011

35 Li, S., Guo, W. & Wu, H. The role of post-translational modifications in the regulation of MCL1. *Cell Signal* **81**, 109933 (2021). https://doi.org/10.1016/j.cellsig.2021.109933

36 Lee, E. F. & Fairlie, W. D. The Structural Biology of Bcl-xL. *Int J Mol Sci* **20** (2019). https://doi.org/10.3390/ijms20092234

37 Lewis, A., Hayashi, T., Su, T. P. & Betenbaugh, M. J. Bcl-2 family in inter-organelle modulation of calcium signaling; roles in bioenergetics and cell survival. *J Bioenerg Biomembr* **46**, 1-15 (2014). https://doi.org/10.1007/s10863-013-9527-7

38 Plotz, M. *et al.* Mutual regulation of Bcl-2 proteins independent of the BH3 domain as shown by the BH3-lacking protein Bcl-x(AK). *PLoS One* **7**, e34549 (2012). https://doi.org/10.1371/journal.pone.0034549

39 Li, M., Wang, D., He, J., Chen, L. & Li, H. Bcl-XL: A multifunctional anti-apoptotic protein. *Pharmacol Res* **151**, 104547 (2020). https://doi.org/10.1016/j.phrs.2019.104547

40 Williams, M. M. *et al.* Key Survival Factor, Mcl-1, Correlates with Sensitivity to Combined Bcl-2/Bcl-xL Blockade. *Mol Cancer Res* **15**, 259-268 (2017). https://doi.org/10.1158/1541-7786.MCR-16-0280-T

41 Wertz, I. E. *et al.* Sensitivity to antitubulin chemotherapeutics is regulated by MCL1 and FBW7. *Nature* **471**, 110-114 (2011). https://doi.org/10.1038/nature09779

42 Kotschy, A. *et al.* The MCL1 inhibitor S63845 is tolerable and effective in diverse cancer models. *Nature* **538**, 477-482 (2016). https://doi.org/10.1038/nature19830

43 Tse, C. *et al.* ABT-263: a potent and orally bioavailable Bcl-2 family inhibitor. *Cancer Res* **68**, 3421-3428 (2008). https://doi.org/10.1158/0008-5472.CAN-07-5836

44 Barretina, J. *et al.* The Cancer Cell Line Encyclopedia enables predictive modelling of anticancer drug sensitivity. *Nature* **483**, 603-607 (2012). https://doi.org/10.1038/nature11003

45 Ghandi, M. *et al.* Next-generation characterization of the Cancer Cell Line Encyclopedia. *Nature* **569**, 503-508 (2019). https://doi.org/10.1038/s41586-019-1186-3

46 Medina, P. P. *et al.* Frequent BRG1/SMARCA4-inactivating mutations in human lung cancer cell lines. *Hum Mutat* **29**, 617-622 (2008). https://doi.org/10.1002/humu.20730

47 Karnezis, A. N. *et al.* Re-assigning the histologic identities of COV434 and TOV-112D ovarian cancer cell lines. *Gynecol Oncol* **160**, 568-578 (2021). https://doi.org/10.1016/j.ygyno.2020.12.004

48 Yang, W. *et al.* Genomics of Drug Sensitivity in Cancer (GDSC): a resource for therapeutic biomarker discovery in cancer cells. *Nucleic Acids Res* **41**, D955-961 (2013). https://doi.org/10.1093/nar/gks1111

49 Xiang, W., Yang, C. Y. & Bai, L. MCL-1 inhibition in cancer treatment. *Onco Targets Ther* **11**, 7301-7314 (2018). https://doi.org/10.2147/OTT.S146228

50 Song, S. *et al.* Loss of SWI/SNF Chromatin Remodeling Alters NRF2 Signaling in Non-Small Cell Lung Carcinoma. *Mol Cancer Res* **18**, 1777-1788 (2020). https://doi.org/10.1158/1541-7786.MCR-20-0082

51 Orlando, K. A. *et al.* Re-expression of SMARCA4/BRG1 in small cell carcinoma of ovary, hypercalcemic type (SCCOHT) promotes an epithelial-like gene signature through an AP-1-dependent mechanism. *Elife* **9** (2020). https://doi.org/10.7554/eLife.59073

52 Stevens, M. & Oltean, S. Modulation of the Apoptosis Gene Bcl-x Function Through Alternative Splicing. *Front Genet* **10**, 804 (2019). https://doi.org/10.3389/fgene.2019.00804

53 Cancer Genome Atlas Research, N. Integrated genomic analyses of ovarian carcinoma. *Nature* **474**, 609-615 (2011). https://doi.org/10.1038/nature10166

54 Zhang, H. *et al.* Mcl-1 is critical for survival in a subgroup of non-small-cell lung cancer cell lines. *Oncogene* **30**, 1963-1968 (2011). https://doi.org/10.1038/onc.2010.559

55 Raupach, E. A. *et al.* Loss of SMARCA4 Leads to Intron Retention and Generation of Tumor-Associated Antigens in Small Cell Carcinoma of the Ovary, Hypercalcemic Type. *Cancer Res* **85**, 2626-2642 (2025). https://doi.org/10.1158/0008-5472.CAN-24-0044

56 Szlavik, Z. *et al.* Discovery of S64315, a Potent and Selective Mcl-1 Inhibitor. *J Med Chem* **63**, 13762-13795 (2020). https://doi.org/10.1021/acs.jmedchem.0c01234

57 Letai, A. S63845, an MCL-1 Selective BH3 Mimetic: Another Arrow in Our Quiver. *Cancer Cell* **30**, 834-835 (2016). https://doi.org/10.1016/j.ccell.2016.11.016

58 https://clinicaltrials.gov.

59 Hellmuth, S. & Stemmann, O. Separase-triggered apoptosis enforces minimal length of mitosis. *Nature* **580**, 542-547 (2020). https://doi.org/10.1038/s41586-020-2187-y

60 Xue, Y. *et al.* SMARCB1 loss induces druggable cyclin D1 deficiency via upregulation of MIR17HG in atypical teratoid rhabdoid tumors. *J Pathol* **252**, 77-87 (2020). https://doi.org/10.1002/path.5493

61 Dobin, A. *et al.* STAR: ultrafast universal RNA-seq aligner. *Bioinformatics* **29**, 15-21 (2013). https://doi.org/10.1093/bioinformatics/bts635

62 Liao, Y., Smyth, G. K. & Shi, W. featureCounts: an efficient general purpose program for assigning sequence reads to genomic features. *Bioinformatics* **30**, 923-930 (2014). https://doi.org/10.1093/bioinformatics/btt656

63 Langmead, B., Trapnell, C., Pop, M. & Salzberg, S. L. Ultrafast and memory-efficient alignment of short DNA sequences to the human genome. *Genome Biol* **10**, R25 (2009). https://doi.org/10.1186/gb-2009-10-3-r25

64 Le Loarer, F. *et al.* SMARCA4 inactivation defines a group of undifferentiated thoracic malignancies transcriptionally related to BAF-deficient sarcomas. *Nat Genet* **47**, 1200-1205 (2015). https://doi.org/10.1038/ng.3399

65 https://ggplot2.tidyverse.org.

66 Pan, J. *et al.* The ATPase module of mammalian SWI/SNF family complexes mediates subcomplex identity and catalytic activity-independent genomic targeting. *Nat Genet* **51**, 618-626 (2019). https://doi.org/10.1038/s41588-019-0363-5

Figure legends

Figure 1. SMARCA4/2-deficient lung and ovarian cancer cells are selectively sensitive to MCL1 inhibition

a, Volcano plot of DepMap genome-wide CRISPR/Cas9 screens showing differential gene dependency (ΔCERES) between SMARCA4/2-deficient and -proficient NSCLC and ovarian cancer cell lines ($A4/2^{Def}$ vs $A4/2^{Pro}$). All BCL2 family proteins were labeled. **b**, Violin plots showing IC_{50} values (log_2) of MCL1 inhibitors in SMARCA4/2-dual deficient ($A4/2^{Def}$) and -proficient ($A4/2^{Pro}$) lung and ovarian cancer cell lines (the plotted cell lines represent the common set found in both the GDSC and CCLE databases). For AZD5991, $n = 44$ ($A4/2^{Pro}$) vs 7 ($A4/2^{Def}$); for MIM1, $n = 48$ ($A4/2^{Pro}$) vs 10 ($A4/2^{Def}$); for UMI-77, $n = 45$ ($A4/2^{Pro}$) vs 7 ($A4/2^{Def}$). Each point represents a cell line (gray: lung; red: ovary). $^{**}p < 0.01$; $^{***}p < 0.001$, unpaired two-tailed Student's *t*-test. **c–d**, Colony formation (**c**) and immunoblot (**d**) analyses of NSCLC cells expressing control or MCL1 shRNAs. MCL1 knockdown suppressed long-term growth and increased cleaved PARP in SMARCA4/2-deficient H1703 cells but not in proficient H1437 cells. **e–f**, Colony formation (**e**) and immunoblot (**f**) analyses of ovarian cancer cells expressing control or MCL1 shRNAs. SMARCA4/2-deficient SCCOHT-1 and BIN-67 cells were sensitive to MCL1 knockdown, whereas SMARCA4/2-proficient OVCAR4 high-grade serous carcinoma cells were less affected. **g–h**, Colony formation (**g**) and cell viability (**h**) assays showing that SMARCA4/2-deficient NSCLC lines (A427, H661, H1703, H23) were more sensitive to the selective MCL1 inhibitor S63845 than proficient lines (H358, H1437, HCC827). **i**, Tumor growth curves of SMARCA4/2-deficient NSCLC PDX (TM01563) models treated with vehicle or S63845 (25 mg/kg, intraperitoneally, twice weekly). S63845 significantly suppressed tumor growth, $n = 3$ (Vehicle) vs 4 (S63845). Error bars, mean ± s.d.; $^{****}p < 0.0001$, two-way ANOVA. **j–k**, Colony formation (**j**) and cell viability (**k**) assays showing that SMARCA4/2-deficient SCCOHT cells (COV434, SCCOHT-1, BIN-67) were markedly sensitive to S63845 compared with OVCAR4 and FT190 controls. Tumor growth curves of SMARCA4/2-deficient SCCOHT PDX (NRTO-1) models treated with vehicle or S63845 $n = 5$ (Vehicle) vs 5 (S63845), showing significant tumor growth inhibition *in vivo*. Error bars, mean ± s.d.; $^{****}p < 0.0001$, two-way ANOVA.

Figure 2. SMARCA4 re-expression reduces sensitivity to MCL1 inhibition in SMARCA4/2-deficient cells.

a–d, Cell viability (**a, b**), n= 3-6, Error bars, mean ± s.d., colony formation (**c**) and immunoblot (**d**) showing that re-expression of SMARCA4 in SMARCA4/2-deficient NSCLC cells (A427, H1703) conferred resistance to S63845 compared with vector controls. Immunoblot analyses verifying **SMARCA4 restoration in** A427, H1703. **e-g**, Immunoblots of A427 (**e**), H1703 (**f**) and SCCOHT-1 (**g**) cells with or without SMARCA4 treated with or without S63845 for 24 hours.

Figure 3. SMARCA4/2 deficiency mediates synthetic lethality with MCL1 inhibition through downregulation of *BCL-xL* expression.

a, Expression levels of apoptosis-associated genes in ovarian and lung cancer cell lines ± SMARCA4/2 restoration or SMARCA4 knockout. Each dot represents a gene. For all cell lines presented, each condition includes ≥3 technical replicates. Ctrl: control, A2: SMARCA2, A4: SMARCA4. **b**, *BCL2L1* mRNA levels in SCCOHT (n = 13) and HGSC (n = 21) patient tumor samples. $^{***}p < 0.001$, unpaired two-tailed Student's *t*-

test. **c**, Real-time PCR analysis of *BCL-xL* mRNA levels in SMARCA4/2-deficient cell lines expressing vector control (Ctrl), SMARCA4 (A4) or SMARCA2 (A2). $n = 3$, error bars: mean ± s.d., *$p < 0.05$; **$p < 0.01$; ****$p < 0.0001$, Brown-Forsythe and Welch ANOVA. **d**, Immunoblots of indicated cell lines ± SMARCA4 re-expression measuring MCL1 protein levels. Actin was used as a loading control. **e**, Western blots of 21 NSCLC cell lines using antibodies against SMARCA4, SMARCA2, MCL1 and BCL-xL. HSP90 served as loading control. A4: SMARCA4, A4/2: SMARCA4/2, Pro: proficient, Def: deficient, KRAS: KRAS mutation. **f**, Representative genome browser tracks showing SMARCA4/2, H3K27Ac ChIP-Seq and ATAC-Seq peaks at the *BCL2L1* locus in BIN-67 and H1703 cells re-expressing SMARCA4/2.

Figure 4. BCL-xL deficiency predominantly contributes to MCL1 dependency.
a,**b**, Colony formation assays of H1703 (**a**) and SCCOHT-1 (**b**) cells stably expressing pLX304-*GFP*, pLX304-*MCL1*, or pLX304-*BCL-xL*, cultured with indicated concentrations of MCL1 inhibitor for 14 days. **c-h**, Cell viability assays of H1703 (**c**) and SCCOHT-1 (**d**) cells stably expressing pLX304-*GFP*, pLX304-*MCL1*, or pLX304-*BCL-xL*, treated with MCL1 inhibitor for 5 days. $n = 3$, error bars: mean ± s.d. Western blot analysis of H1703 (**e**) and SCCOHT-1 (**f**) cells expressing the indicated constructs and treated with increasing doses of MCL1 inhibitor for 24 hours. Blots were probed for SMARCA4, cleaved PARP, MCL1, BCL-xL, cleaved caspase-3, and HSP90. The ectopically expressed proteins were highlighted by the arrows. Colony formation assay (**g**) and immunoblot analysis (**h**) of H1703 cells expressing the indicated constructs and co-infected with *pLKO* control or *MCL1* 3′UTR-targeting shRNA. Western blots probed with antibodies against SMARCA4, cleaved PARP, MCL1, BCL-xL, and HSP90. **i**, Colony formation assays of A427 and H1703 cells ± SMARCA4 re-expression, cultured with MCL1 inhibitor ± 1 μM WEHI-539 (BCL-xL selective inhibitor) for 14 days. All plates were fixed at the same time.

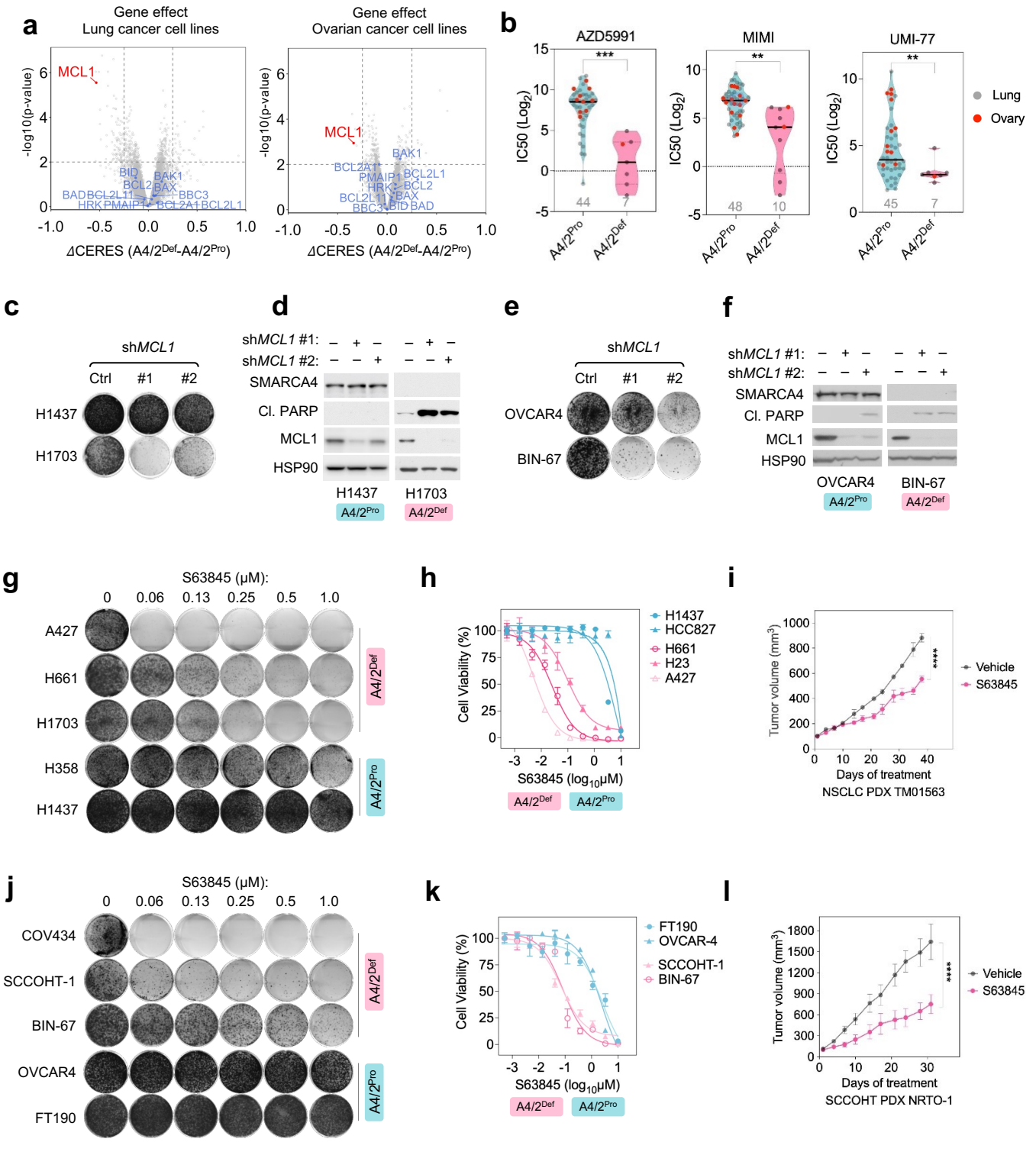
a
Gene effect
Lung cancer cell lines
Gene effect
Ovarian cancer cell lines
-log10(p-value)
MCL1
BID
BCL2
BAK1
BAX
BAD
BCL2L11
BBC3
HRK
PMAIP1
BCL2A1
BCL2L1
ΔCERES (A4/2Def-A4/2Pro)
b
AZD5991
MIMI
UMI-77
IC50 (Log2)
***
**
**
44
7
48
10
45
7
A4/2Pro
A4/2Def
Lung
Ovary
c
shMCL1
Ctrl
#1
#2
H1437
H1703
d
shMCL1 #1:
shMCL1 #2:
SMARCA4
Cl. PARP
MCL1
HSP90
H1437
H1703
A4/2Pro
A4/2Def
e
shMCL1
Ctrl
#1
#2
OVCAR4
BIN-67
f
shMCL1 #1:
shMCL1 #2:
SMARCA4
Cl. PARP
MCL1
HSP90
OVCAR4
BIN-67
A4/2Pro
A4/2Def
g
S63845 (μM):
0
0.06
0.13
0.25
0.5
1.0
A427
H661
H1703
H358
H1437
A4/2Def
A4/2Pro
h
Cell Viability (%)
S63845 (log10μM)
H1437
HCC827
H661
H23
A427
A4/2Def
A4/2Pro
i
Tumor volume (mm3)
Days of treatment
NSCLC PDX TM01563
****
Vehicle
S63845
j
S63845 (μM):
0
0.06
0.13
0.25
0.5
1.0
COV434
SCCOHT-1
BIN-67
OVCAR4
FT190
A4/2Def
A4/2Pro
k
Cell Viability (%)
S63845 (log10μM)
FT190
OVCAR-4
SCCOHT-1
BIN-67
A4/2Def
A4/2Pro
l
Tumor volume (mm3)
Days of treatment
SCCOHT PDX NRTO-1
****
Vehicle
S63845

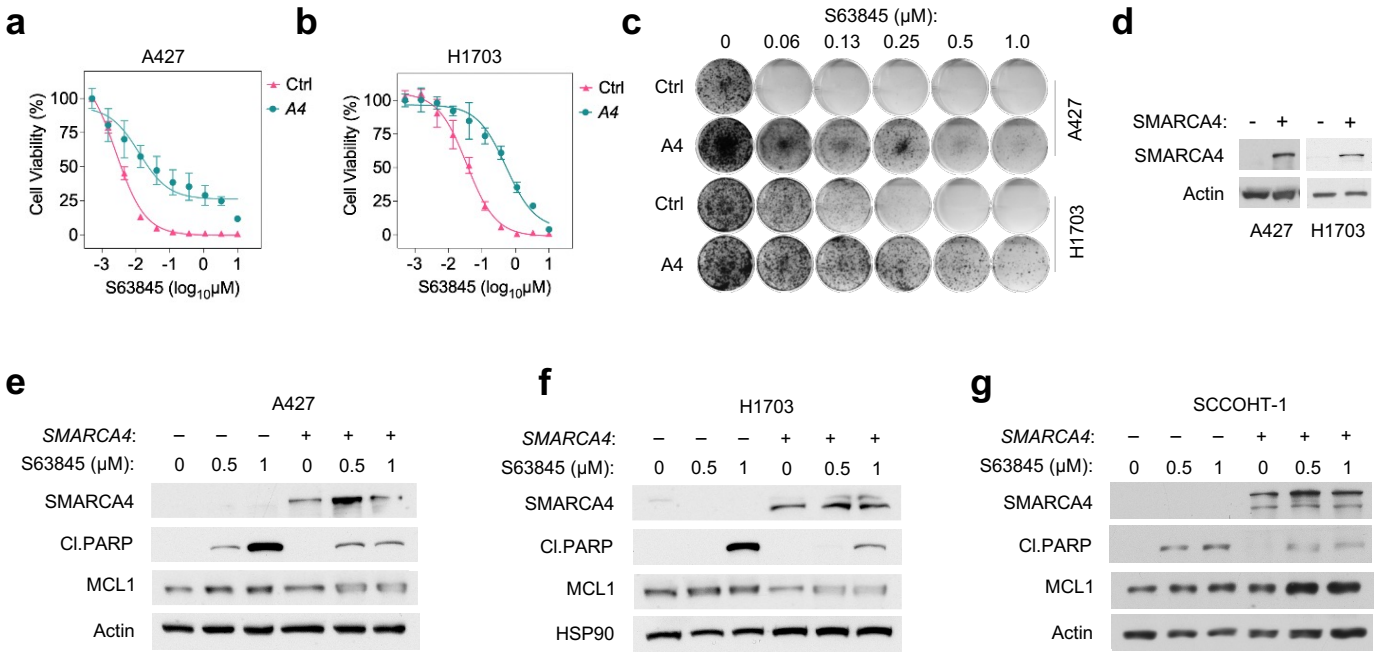
a
A427
Cell Viability (%)
100
75
50
25
0
-3 -2 -1 0 1
S63845 (log10μM)
Ctrl
A4
b
H1703
Cell Viability (%)
100
75
50
25
0
-3 -2 -1 0 1
S63845 (log10μM)
Ctrl
A4
c
S63845 (μM):
0 0.06 0.13 0.25 0.5 1.0
Ctrl
A4
Ctrl
A4
A427
H1703
d
SMARCA4: - + - +
SMARCA4
Actin
A427 H1703
e
A427
SMARCA4: – – – + + +
S63845 (μM): 0 0.5 1 0 0.5 1
SMARCA4
Cl.PARP
MCL1
Actin
f
H1703
SMARCA4: – – – + + +
S63845 (μM): 0 0.5 1 0 0.5 1
SMARCA4
Cl.PARP
MCL1
HSP90
g
SCCOHT-1
SMARCA4: – – – + + +
S63845 (μM): 0 0.5 1 0 0.5 1
SMARCA4
Cl.PARP
MCL1
Actin

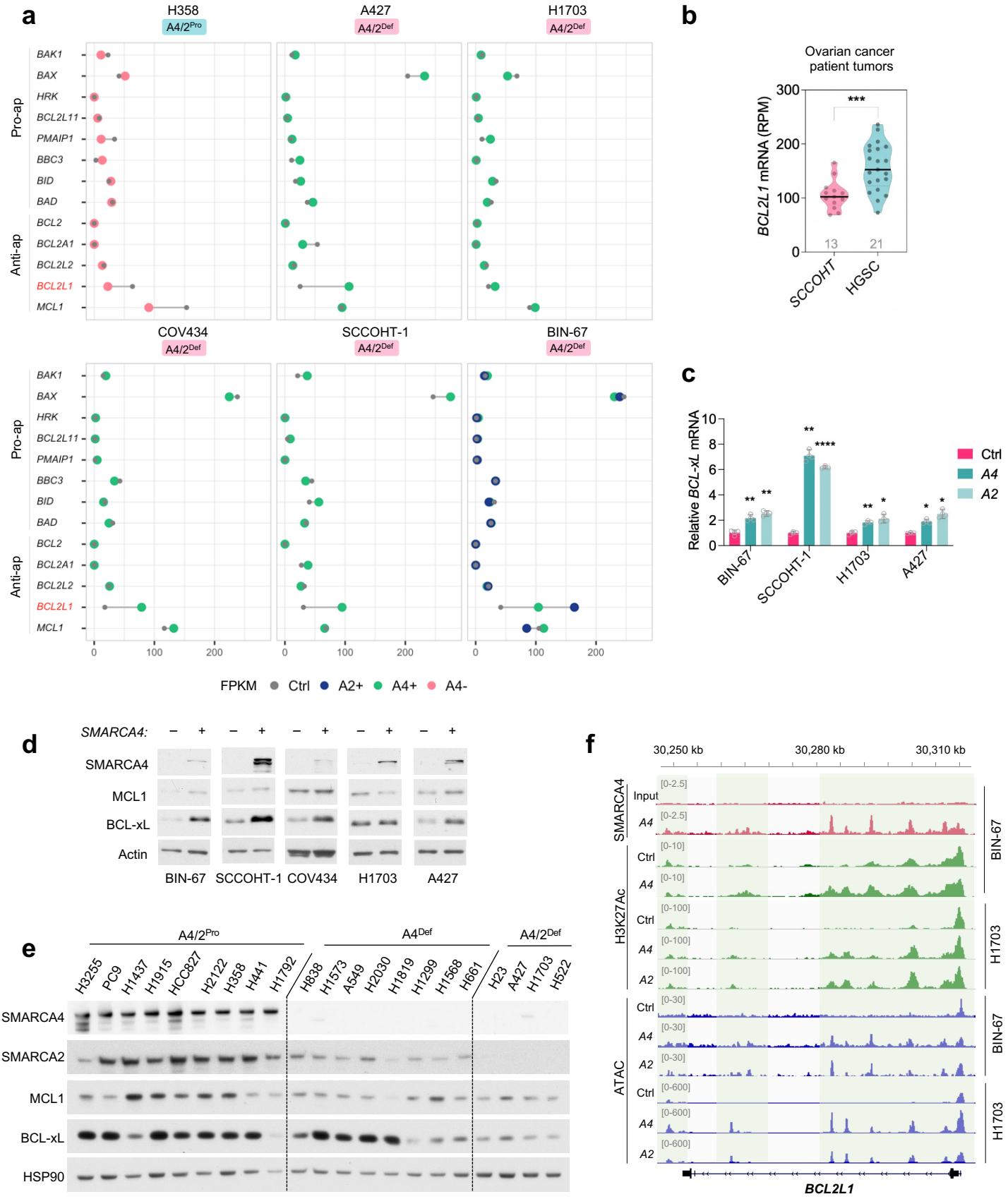
a
H358
A4/2Pro
A427
A4/2Def
H1703
A4/2Def
COV434
A4/2Def
SCCOHT-1
A4/2Def
BIN-67
A4/2Def
Pro-ap
Anti-ap
BAK1
BAX
HRK
BCL2L11
PMAIP1
BBC3
BID
BAD
BCL2
BCL2A1
BCL2L2
BCL2L1
MCL1
0
100
200
FPKM
Ctrl
A2+
A4+
A4-
b
Ovarian cancer patient tumors
BCL2L1 mRNA (RPM)
300
200
100
0
***
13
21
SCCOHT
HGSC
c
Relative BCL-xL mRNA
10
8
6
4
2
0
**
**
**
****
**
*
*
*
BIN-67
SCCOHT-1
H1703
A427
Ctrl
A4
A2
d
SMARCA4:
– + – + – + – + – +
SMARCA4
MCL1
BCL-xL
Actin
BIN-67
SCCOHT-1
COV434
H1703
A427
e
A4/2Pro
A4Def
A4/2Def
H3255
PC9
H1437
H1915
HCC827
H2122
H358
H441
H1792
H838
H1573
A549
H2030
H1819
H1299
H1568
H661
H23
A427
H1703
H522
SMARCA4
SMARCA2
MCL1
BCL-xL
HSP90
f
30,250 kb
30,280 kb
30,310 kb
SMARCA4
Input
A4
H3K27Ac
Ctrl
A4
A2
ATAC
Ctrl
A4
A2
[0-2.5]
[0-10]
[0-100]
[0-30]
[0-600]
BIN-67
H1703
BCL2L1

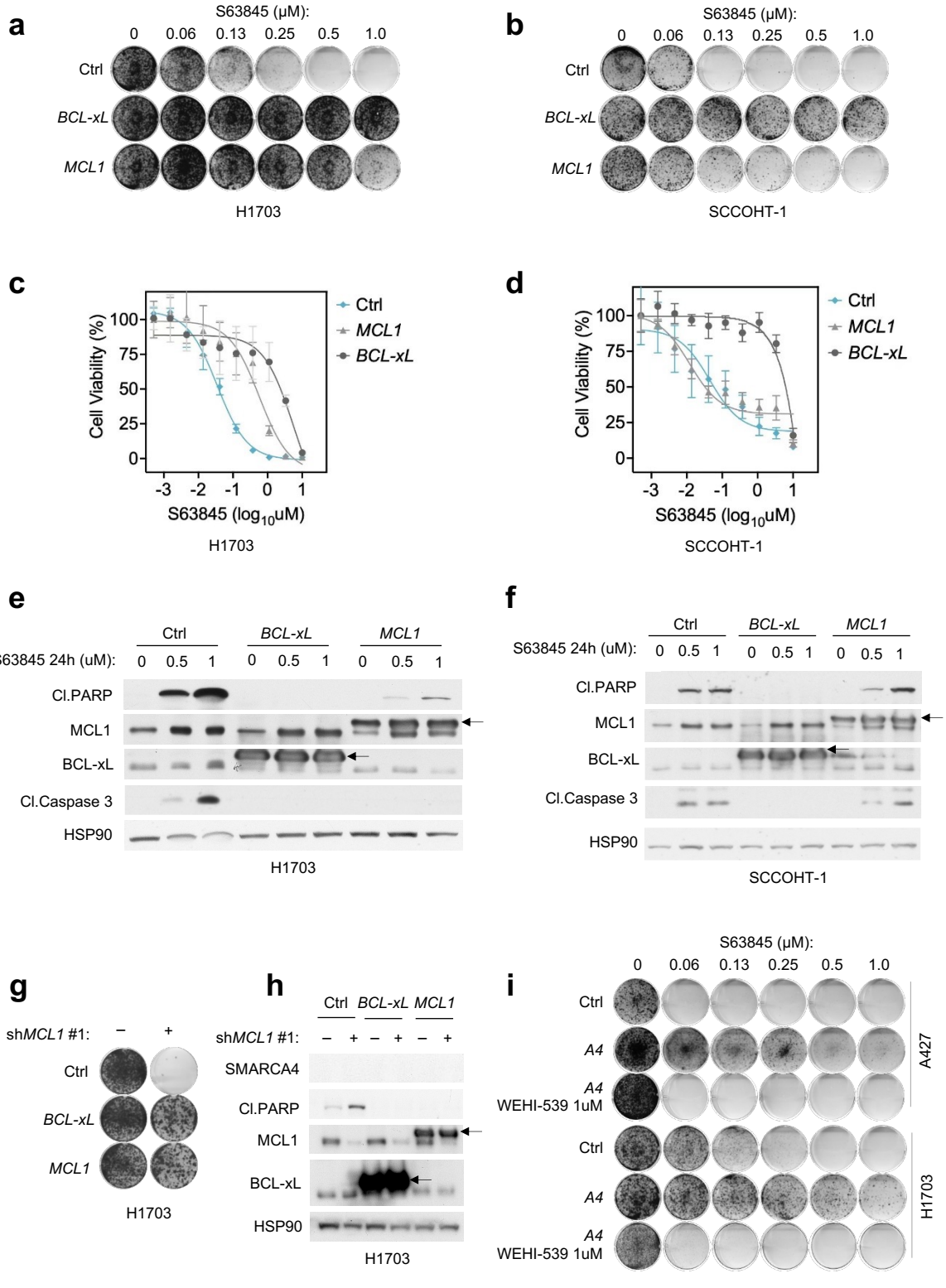
a
S63845 (μM):
0 0.06 0.13 0.25 0.5 1.0
Ctrl
BCL-xL
MCL1
H1703
b
S63845 (μM):
0 0.06 0.13 0.25 0.5 1.0
Ctrl
BCL-xL
MCL1
SCCOHT-1
c
Cell Viability (%)
100 75 50 25 0
-3 -2 -1 0 1
S63845 (log10uM)
Ctrl
MCL1
BCL-xL
H1703
d
Cell Viability (%)
100 75 50 25 0
-3 -2 -1 0 1
S63845 (log10uM)
Ctrl
MCL1
BCL-xL
SCCOHT-1
e
Ctrl
BCL-xL
MCL1
S63845 24h (uM):
0 0.5 1 0 0.5 1 0 0.5 1
Cl.PARP
MCL1
BCL-xL
Cl.Caspase 3
HSP90
H1703
f
Ctrl
BCL-xL
MCL1
S63845 24h (uM):
0 0.5 1 0 0.5 1 0 0.5 1
Cl.PARP
MCL1
BCL-xL
Cl.Caspase 3
HSP90
SCCOHT-1
g
shMCL1 #1: – +
Ctrl
BCL-xL
MCL1
H1703
h
Ctrl
BCL-xL
MCL1
shMCL1 #1: – + – + – +
SMARCA4
Cl.PARP
MCL1
BCL-xL
HSP90
H1703
i
S63845 (μM):
0 0.06 0.13 0.25 0.5 1.0
Ctrl
A4
A4
WEHI-539 1uM
A427
Ctrl
A4
A4
WEHI-539 1uM
H1703